Science Advances
AAAS

advances.sciencemag.org/cgi/content/full/6/50/eabc2697/DC1

Supplementary Materials for

Efficient aortic lymphatic drainage is necessary for atherosclerosis regression induced by ezetimibe

Kim Pin Yeo, Hwee Ying Lim, Chung Hwee Thiam, Syaza Hazwany Azhar, Caris Tan, Ya Tang, Wei Qiang See, Xuan Han Koh, Ming Hao Zhao, Meow Ling Phua, Akhila Balachander, Yingrou Tan, Sheau Yng Lim, Hui Shang Chew, Lai Guan Ng, Veronique Angeli*

*Corresponding author. Email: micva@nus.edu.sg

Published 11 December 2020, *Sci. Adv.* **6**, eabc2697 (2020)
DOI: 10.1126/sciadv.abc2697

The PDF file includes:

Other Supplementary Material for this manuscript includes the following:

(available at advances.sciencemag.org/cgi/content/full/6/50/eabc2697/DC1)

fig. S1

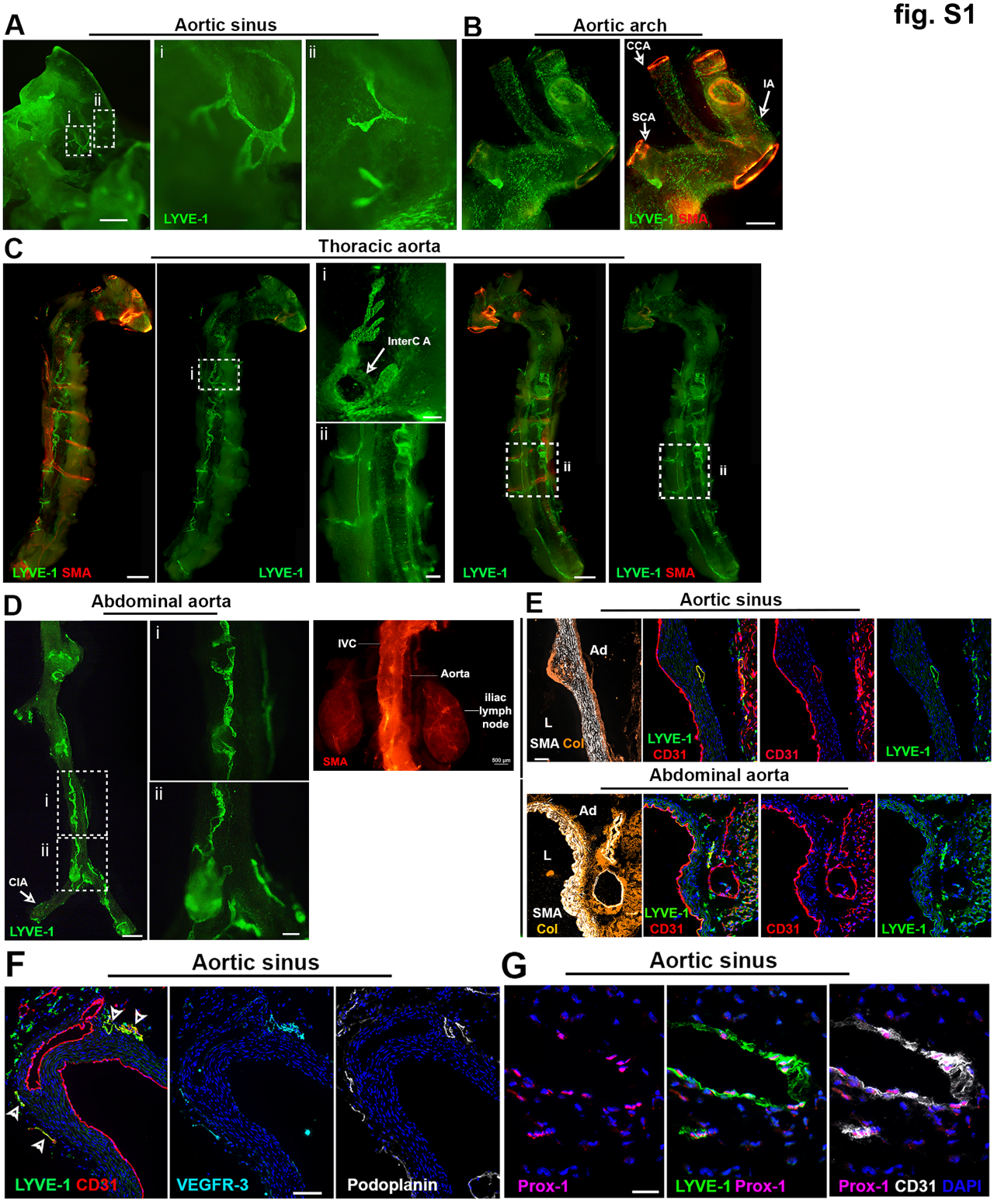

Figure S1. Topography of lymphatic vessels in normocholesterolemic WT aorta. Immunoreactivity for LYVE-1 (green) and SMA (red) was examined in whole-mount (A) aortic sinus, (B) aortic arch, (C) thoracic aorta and (D) abdominal aorta of 6 weeks old WT mouse. Innominate artery (IA), common carotid artery (CCA), subclavian artery (SCA), intercostal artery (InterC A), inferior vena cava (IVC) and common iliac artery (CIA).

(E) Immunoreactivity for LYVE-1^{+} (green) and CD31^{+} (red) lymphatic was examined in aortic sinus and abdominal aorta cross-sections. Lymphatic vessels expressed LYVE-1 and CD31 while blood vessels expressed only CD31. Type I collagen (COLI) and SMA staining identified the adventitial and medial layers of the aorta, respectively. (F) Lymphatic vessels identity was further confirmed with other lymphatic markers, VEGFR-3 (cyan) and podoplanin (white) and (G) prox-1 (purple). The scale bar represents (A) 1 mm, magnified inset (i) 100 μm, (ii) 200 μm; (B) 500 μm; (C) 1 mm, magnified inset (i) 200 μm, (ii) 500 μm; (D) 1mm, magnified insets (i) and (ii) 200 μm; (E) 100 μm and (F-G) 100 μm.

fig. S2

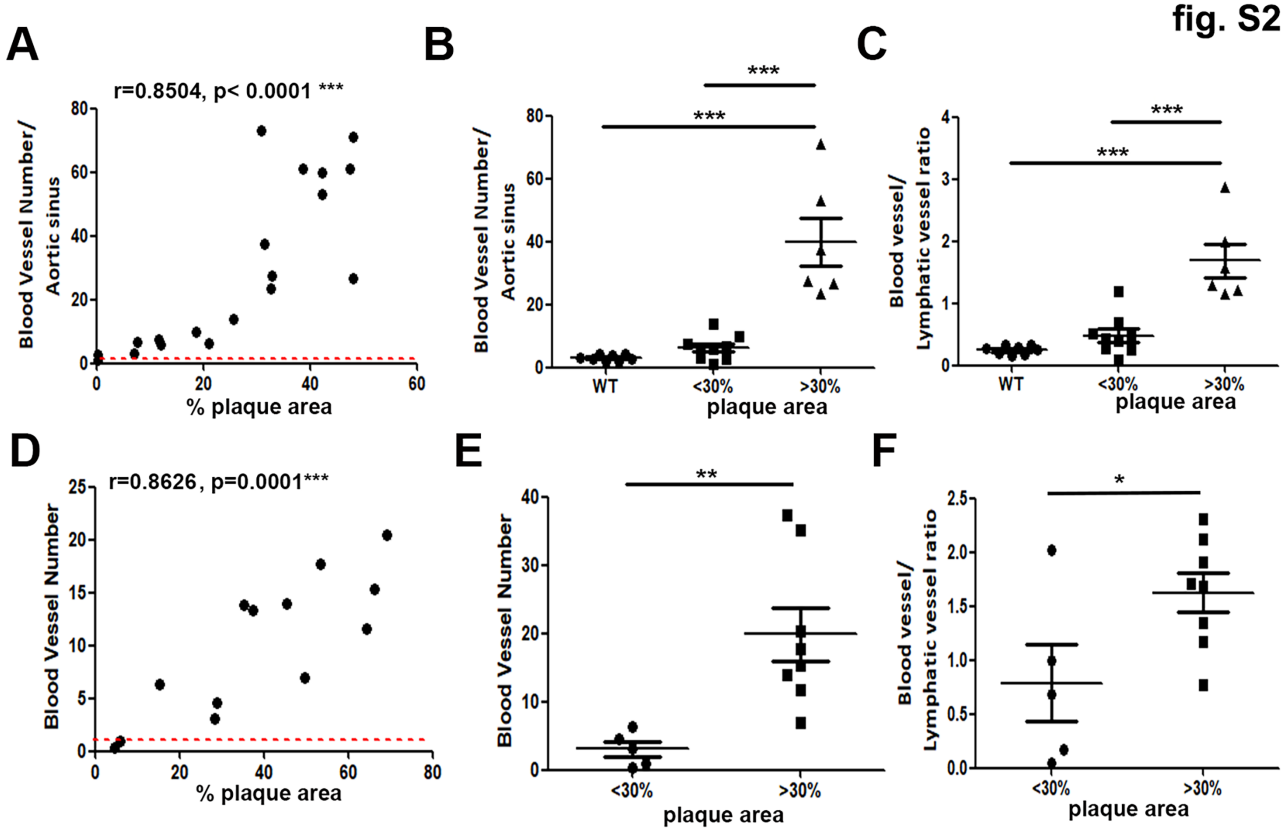

Figure S2. Remodelling of adventitial vasa vasorum in *Apoe*$^{-/-}$. (A) Correlation of blood vessel numbers per aortic sinus with percentage of plaque area was analysed. Spearman's correlation r= 0.8504; *** *p* value< 0.0001. (B) Quantification of blood vessel numbers (C) blood to lymphatic vessel ratio in aortic sinus of WT and *Apoe*$^{-/-}$ mice with less or more than 30% of plaque area were quantified. (D) Correlation of blood vessel numbers per abdominal aorta cross section with percentage of plaque area was assessed. Spearman's correlation r= 0.8626; *** *p* value< 0.0001. (E) Quantification of blood vessel numbers (F) blood to lymphatic vessel ratio of abdominal aorta cross sections in WT and *Apoe*$^{-/-}$ mice with less or more than 30% of plaque area were quantified. Each point represents one mouse and at least 5 mice were included per group. Data were expressed as mean ± SEM. One-way ANOVA was used for multiple group comparisons otherwise student *t* test was used; * *p* value< 0.05, ** *p* value< 0.01, *** *p* value< 0.0001.

fig. S3

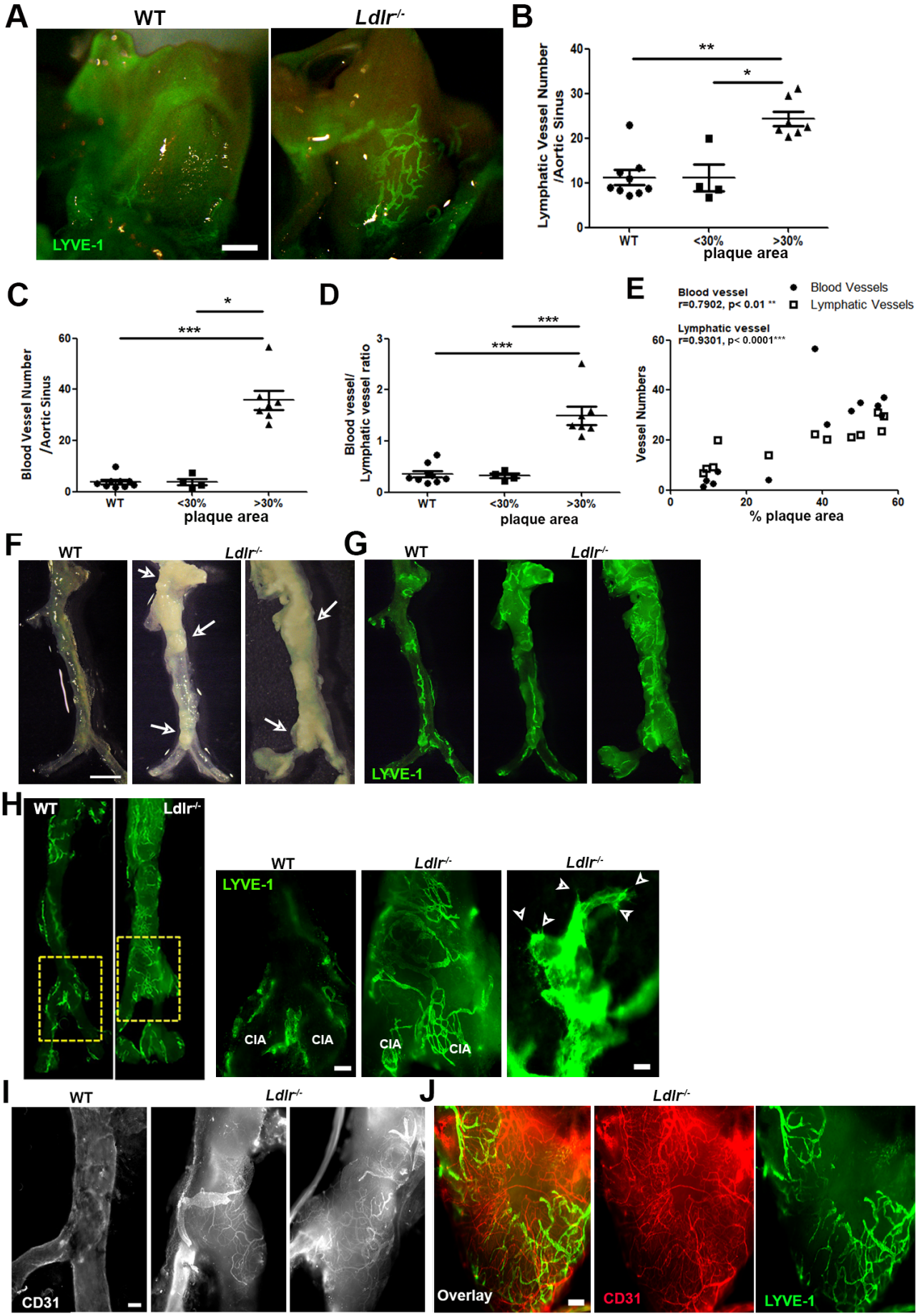
A
WT
Ldlr-/-
LYVE-1
B
Lymphatic Vessel Number /Aortic Sinus
**
*
WT
<30%
>30%
plaque area
C
Blood Vessel Number /Aortic Sinus
*
***
WT
<30%
>30%
plaque area
D
Blood vessel/ Lymphatic vessel ratio
***
***
WT
<30%
>30%
plaque area
E
Blood vessel
r=0.7902, p< 0.01 **
Blood Vessels
Lymphatic Vessels
Lymphatic vessel
r=0.9301, p< 0.0001***
Vessel Numbers
% plaque area
F
WT
Ldlr-/-
G
WT
Ldlr-/-
LYVE-1
H
WT
Ldlr-/-
WT
Ldlr-/-
Ldlr-/-
LYVE-1
CIA
CIA
CIA
CIA
I
WT
Ldlr-/-
CD31
J
Ldlr-/-
Overlay
CD31
LYVE-1

Figure S3. Remodelling of adventitial lymphatic and blood vasa vasorum in *Ldlr*$^{-/-}$ mice. (A) Immunoreactivity for LYVE-1 (green) in aortic sinus whole-mounts from 40-week old WT and *Ldlr*$^{-/-}$ mice. The scale bar represents 500 μm. (B) Quantification of lymphatic vessel numbers, (C) blood vessel numbers and (D) blood to lymphatic vessel ratio per aortic sinus of WT and *Ldlr*$^{-/-}$ mice with less or more than 30% of plaque area were analysed. (E) Correlation of blood and lymphatic vessel numbers per aortic sinus with percentage of plaque area was assessed. Spearman's correlation r= 0.7902; ** *p* value< 0.01 for blood vessel and Spearman's correlation r= 0.9301; *** *p* value< 0.0001 for lymphatic vessel. (F) Bright field of abdominal aorta in WT and *Ldlr*$^{-/-}$ mice with different plaque burden. Arrows indicated atherosclerotic plaque. (G) Immunoreactivity for LYVE-1 (green) in abdominal aorta from 46 weeks old WT and *Ldlr*$^{-/-}$ mice with different plaque burden. The scale bar represents 1 mm. (H) Immunoreactivity for (H) LYVE-1 (green) and (I) CD31 (white) was examined in the WT and *Ldlr*$^{-/-}$ abdominal aorta near iliac bifurcation. The scale bar represents 200 μm. Arrowheads indicate lymphatic sprouts. The scale bar represents 20 μm. (J) Immunoreactivity for LYVE-1 (green) and CD31 (red) was examined in *Ldlr*$^{-/-}$ abdominal aorta near renal arteries. The scale bar represents 200 μm. Each point represents one mouse and at least 4 mice per group were included. Data were expressed as mean ± SEM. One-way ANOVA was used for multiple group comparisons; * *p* value< 0.05, ** *p* value< 0.01, *** *p* value< 0.0001.

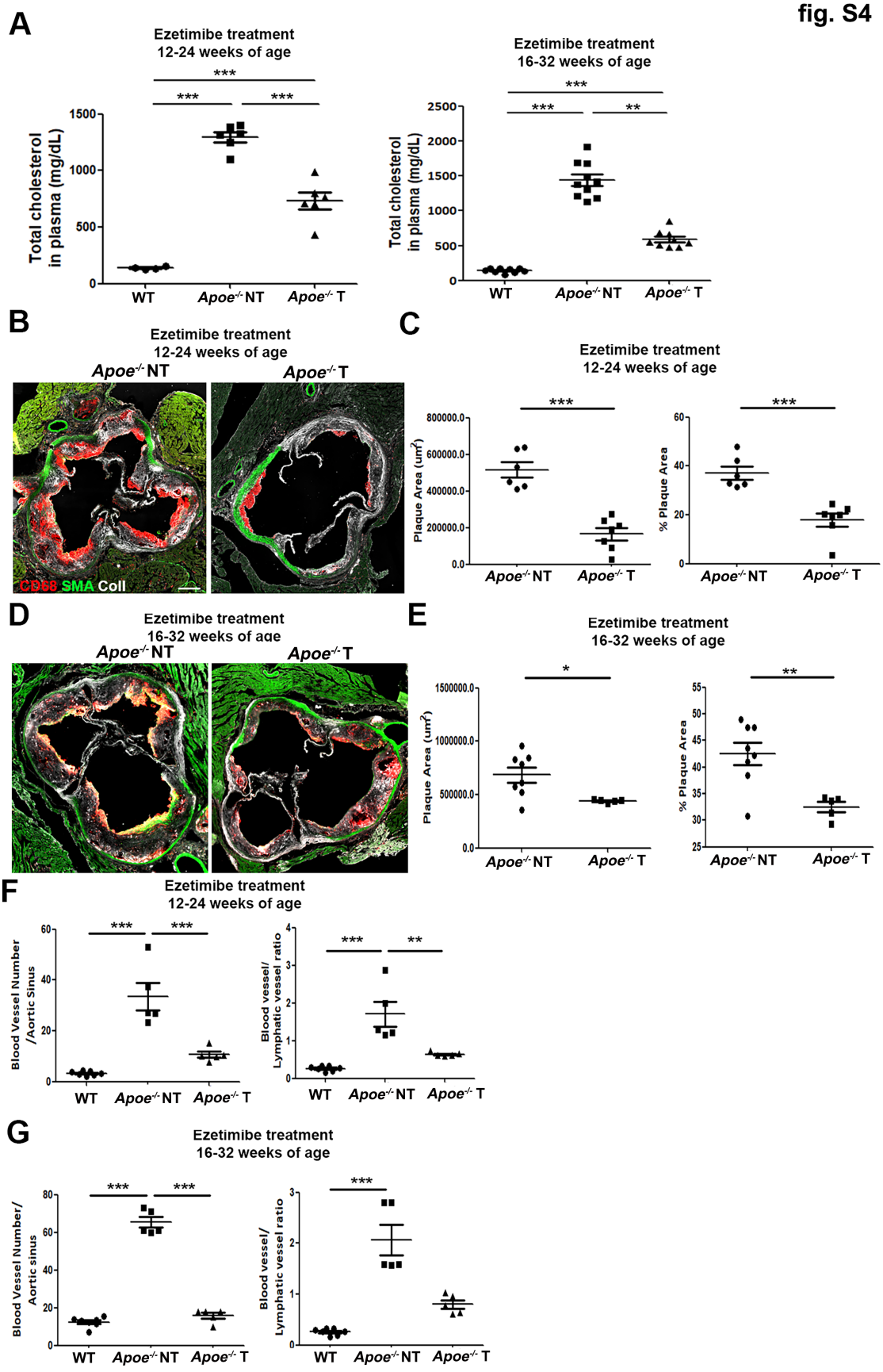

Figure S4. Effects of ezetimibe treatment on plasma cholesterol, atherosclerosis and adventitial vasa vasorum. (A) Total cholesterol levels were measured in the plasma of WT and *Apoe*$^{-/-}$ mice after 12 weeks

and 16 weeks of treatment with vehicle (non-treated, NT) or ezetimibe (treated, T). (B) Immunoreactivity for CD68 (red), COLI (white) and smooth muscle actin (SMA) (green) in aortic sinus cross-sections was examined after 12 weeks of treatment. (C) Plaque area and percentage of plaque area after 12 weeks of treatment were quantified. (D) Immunoreactivity for CD68 (red), COLI (white) and smooth muscle actin (SMA) (green) in aortic sinus cross-sections was examined after 16 weeks of treatment. (E) Plaque area and percentage of plaque area after 16 weeks of treatment were quantified. (F) Blood vessel numbers and blood to lymphatic vessel ratio per aortic sinus after (F) 12 weeks and (G) 16 weeks of vehicle or ezetimibe treatments were quantified. Data were expressed as mean ± SEM with n= 6-7 mice. Each point represents one mouse. At least 8 sections per aortic sinus cross-sections were quantified and each section was 45 μm apart. One-way ANOVA was used for multiple group comparisons and student *t* test was used for 2 groups comparison and; * *p* value< 0.05, ** *p* value< 0.01, *** *p* value< 0.001.

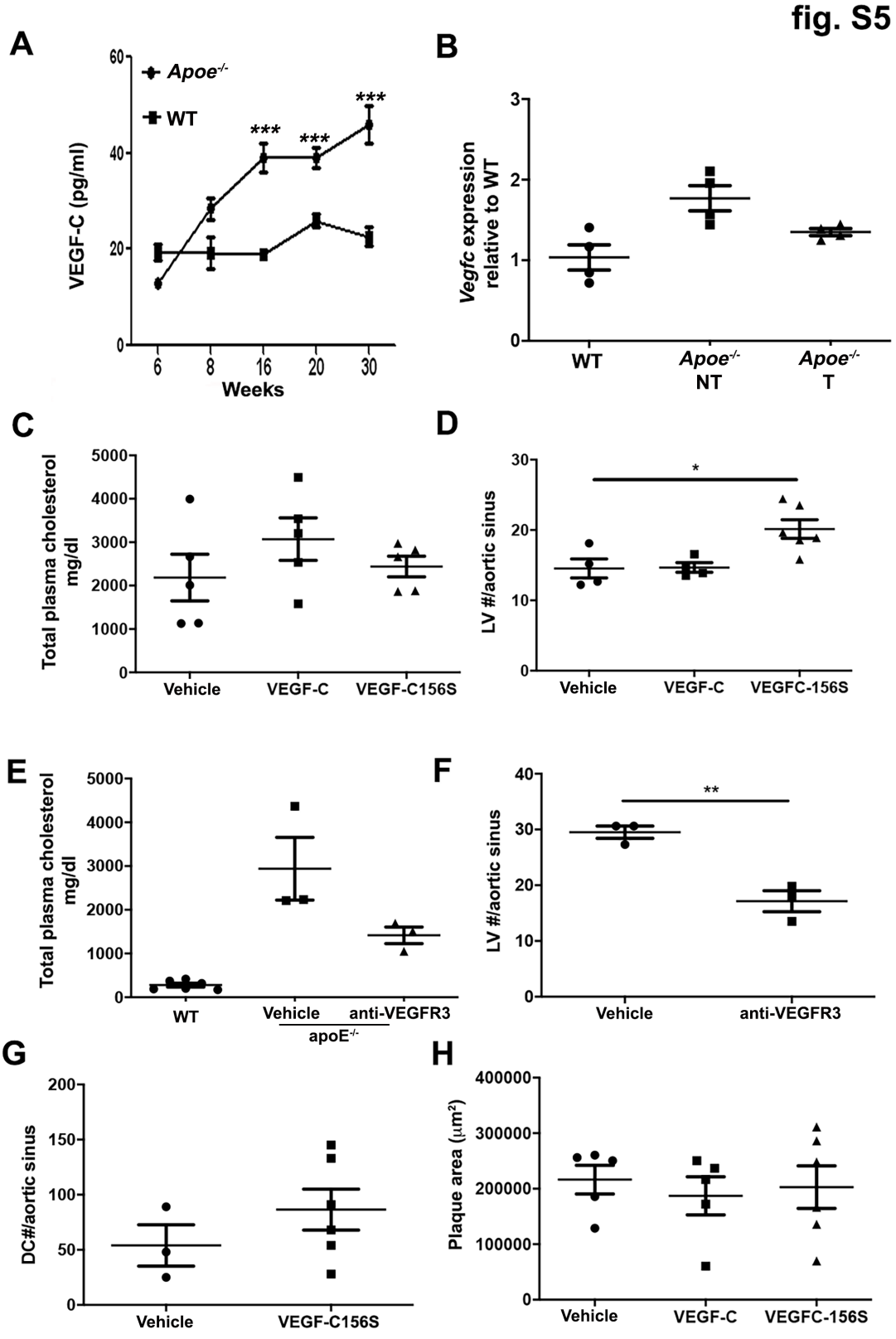

Figure S5. Effect of manipulating VEGF-C activity on lymphatic number and plaque area. (A) VEGF-C in plasma of *Apoe*$^{-/-}$ and WT mice was measured by ELISA. (B) Quantitative real-time PCR analysis of *vegf-c* gene was performed on thoracic and abdominal aorta from 24-week old WT and *Apoe*$^{-/-}$ mice treated with vehicle (non-treated, NT) or ezetimibe (treated, T). (C) Total plasma cholesterol levels and (D) lymphatic vessels

number per aortic sinus were assessed in 17 week-old *Apoe*$^{-/-}$ mice after 10-week administration with PBS, VEGF-C or VEGFC-156S. (E) Total plasma cholesterol levels and (F) lymphatic vessels number per aortic sinus were assessed in 20 week-old *Apoe*$^{-/-}$ mice after 12-week administration with VEGFR-3 blocking antibody or vehicle (PBS). (G) Number of adventitial CD11c+MHCII+ DCs and total atherosclerotic plaque in aortic sinus were assessed in 17-week old *Apoe*$^{-/-}$ mice after 10-week administration with vehicle (PBS) or VEGFC-156S. Data were expressed as mean ± SEM with n= 3-5 mice. Each point represents one mouse. One-way ANOVA was used for multiple group comparisons. Mann-Whitney *U* test and Student *t* test were both employed for 2 groups comparison; * p value< 0.05 and *** p value< 0.001.

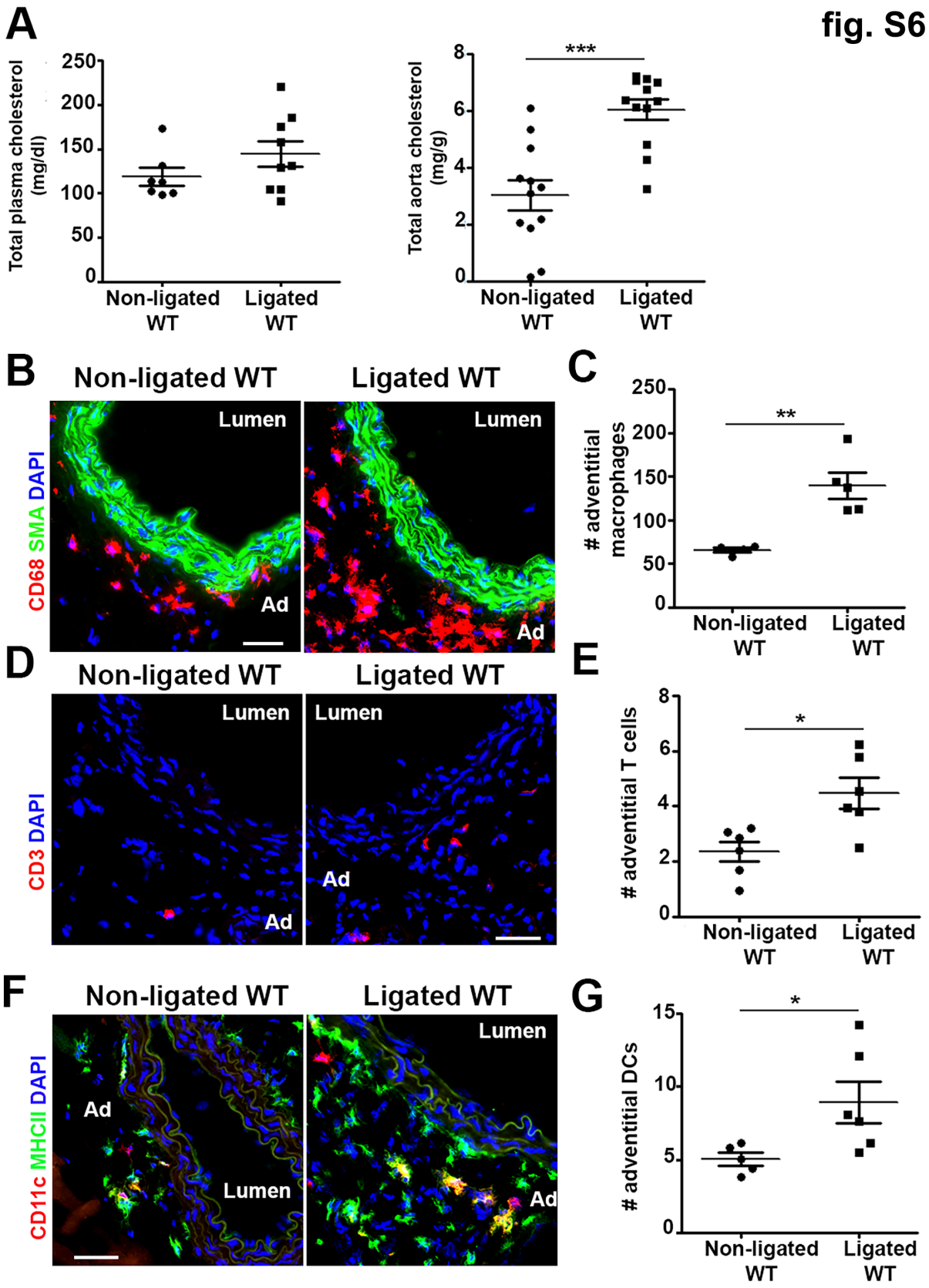

Figure S6. Consequence of aortic lymphatic ligation on normocholesterolemic WT aorta. (A) Total cholesterol levels in the plasma and abdominal aortae from non-ligated and ligated WT mice were assessed.

Immunoreactivity for (B) $CD68^+$ (red) macrophages, (D) $CD3^+$ (red) T cells and (F) $CD11c^+$ (red) $MHCII^+$ (green) DCs was examined in the abdominal aorta from non-ligated and ligated WT mice. The scale bar represents 200 μm. Number of (C) adventitial macrophages, (E) T cells and (G) DCs per abdominal aorta cross-sections from non-ligated and ligated WT mice were quantified. Data were expressed as mean ± SEM with n=4-13 mice. Each point represents one mouse. Mann-Whitney *U* test and Student *t* test were both employed; * *p* value< 0.05, ** *p* value< 0.01, *** *p* value< 0.001.

fig. S7

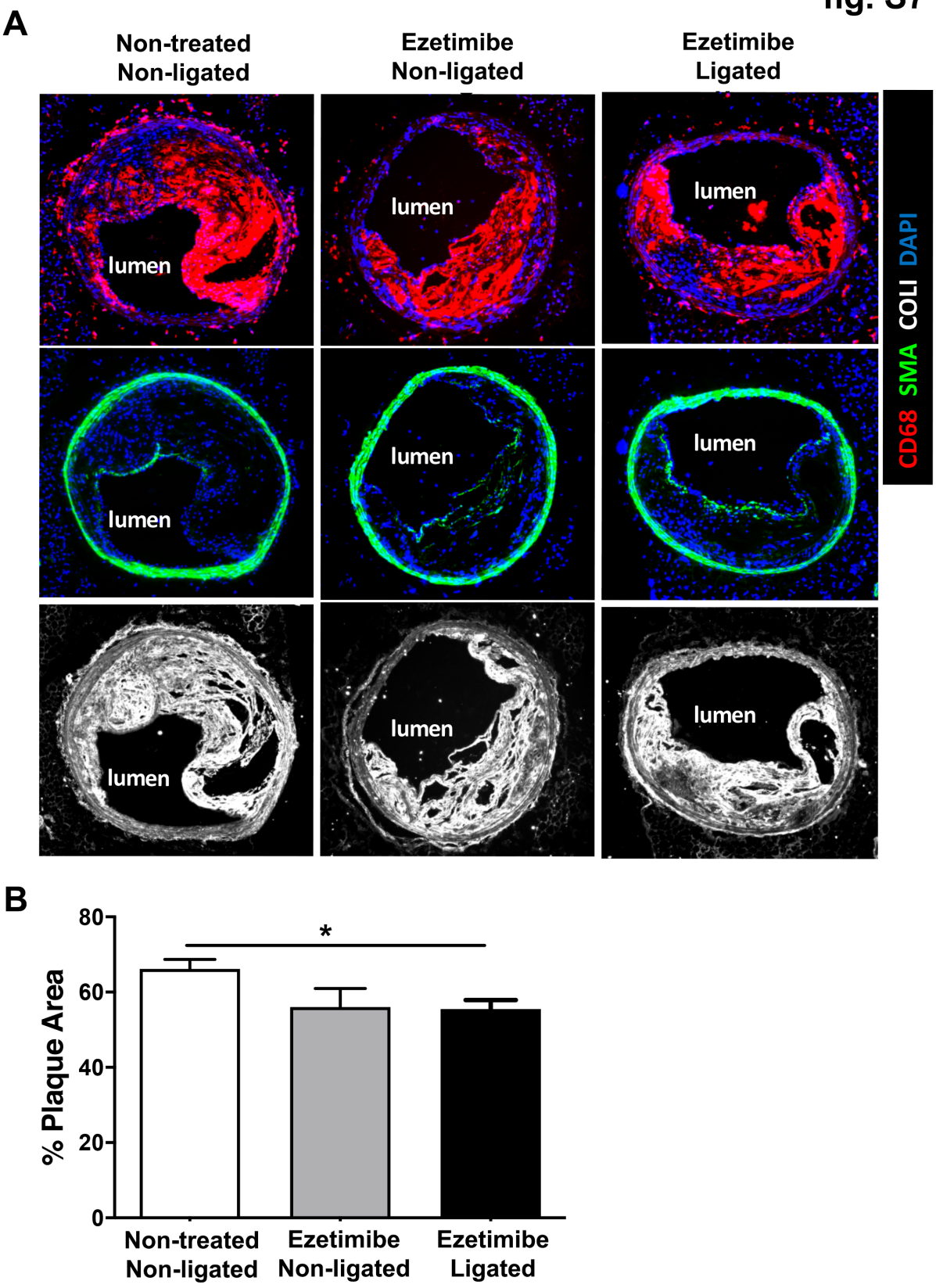

Figure S7. Effect of lymphatic ligation on atherosclerosis in innominate aorta. (A) Immunoreactivity for CD68 (red), COLI (white) and smooth muscle actin (SMA) (green) in innominate artery cross-sections from non-ligated NT *Apoe*$^{-/-}$, non-ligated T *Apoe*$^{-/-}$, and ligated T *Apoe*$^{-/-}$ was examined. The scale bar represents

100 μm. (B) Total plaque area of innominate artery from non-ligated NT *Apoe*$^{-/-}$, non-ligated T *Apoe*$^{-/-}$, and ligated T *Apoe*$^{-/-}$ was quantified. Data were expressed as mean ± SEM with n=7-8 mice; * *p* value< 0.05.

Video 1. Three-dimensional distribution of the lymphatic vessels in abdominal aorta.

Video 2. Drainage of macromolecule from aorta to the renal lymph node. Representative video of FITC-labelled dextran draining route upon its injection on the aortic adventitia.